

# Learning a Hierarchical Compositional Shape Vocabulary for Multi-class Object Representation

Sanja Fidler, *Member, IEEE*, Marko Boben, and Aleš Leonardis, *Member, IEEE*

**Abstract**—Hierarchies allow feature sharing between objects at multiple levels of representation, can code exponential variability in a very compact way and enable fast inference. This makes them potentially suitable for learning and recognizing a higher number of object classes. However, the success of the hierarchical approaches so far has been hindered by the use of hand-crafted features or predetermined grouping rules. This paper presents a novel framework for *learning* a hierarchical compositional shape vocabulary for representing multiple object classes. The approach takes simple contour fragments and learns their frequent spatial configurations. These are recursively combined into increasingly more complex and class-specific shape compositions, each exerting a high degree of shape variability. At the top-level of the vocabulary, the compositions are sufficiently large and complex to represent the whole shapes of the objects. We learn the vocabulary layer after layer, by gradually increasing the size of the window of analysis and reducing the spatial resolution at which the shape configurations are learned. The lower layers are learned jointly on images of all classes, whereas the higher layers of the vocabulary are learned incrementally, by presenting the algorithm with one object class after another. The experimental results show that the learned multi-class object representation scales favorably with the number of object classes and achieves a state-of-the-art detection performance at both, faster inference as well as shorter training times.

**Index Terms**—Hierarchical representations, compositional hierarchies, unsupervised hierarchical structure learning, multiple object class recognition and detection, modeling object structure.



## 1 INTRODUCTION

VISUAL categorization of objects has been an area of active research in the vision community for decades. Ultimately, the goal is to recognize and detect an increasing number of object classes in images within an acceptable time frame. The problem entangles three highly interconnected issues: the internal object **representation** which should compactly capture the high visual variability of objects and generalize well over each class, means of **learning** the representation from a set of images with as little supervision as possible, and an effective **inference** algorithm that robustly matches the object representation against the image.

Using vocabularies of visual features has been a popular choice of object class representation and has yielded some of the most successful performances for object detection to date [1], [2], [3], [4], [5], [6]. However, the majority of these works are currently using flat coding schemes where each object is represented with either no structure at all by using a bag-of-words model or only simple geometry induced over a set of intermediately complex object parts. In this paper, our aim is to model the *hierarchical compositional structure* of the objects and do so for multiple object classes.

Modeling structure (geometry of objects) is important for several reasons. Firstly, since objects within a class have usually distinctive and similar shape, it allows for

an efficient shape parametrization with good generalization capabilities. It further enables us to *parse* objects into meaningful components which is of particular importance in robotic applications where the task is not only to detect objects but also to execute higher-level cognitive tasks (manipulations, grasping, etc). Thirdly, by inducing the structure over the features the representation becomes more robust to background clutter.

Hierarchies incorporate structural dependencies among the features at multiple levels: objects are defined in terms of parts, which are further composed from a set of simpler constituents, etc [7], [8], [9], [10], [11], [12], [13]. Such architectures allow sharing of features between the visually similar as well as dissimilar classes at multiple levels of specificity [14], [11], [15], [12], [16]. Sharing of features means sharing common computations and increasing the speed of the joint detector [2]. More importantly, shared features lead to better generalization [2] and can play an important role of regularization in learning of novel classes with few training examples. Furthermore, since each feature in the hierarchy recursively models certain variance over its parts, it captures a high structural variability and consequently a smaller number of features are needed to represent each class.

Learning of feature vocabularies without or with little supervision is of primary importance in multi-class object representation. By learning, we minimize the amount of time of human involvement in object labeling [10], [17] and avoid bias of pre-determined grouping rules or manually crafted features [18], [19], [20], [21]. Second, learning the representation statistically yields features

• S. Fidler is with University of Toronto, Canada, M. Boben and A. Leonardis are with University of Ljubljana, Slovenia. A. Leonardis is also affiliated with University of Birmingham, UK.  
E-mail: fidler@cs.toronto.edu, {marko.boben, ales.leonardis}@fri.uni-lj.si

most shareable between the classes, which may not be well predicted by human labelers [22]. However, the complexity of *learning the structure* of a hierarchical representation bottom-up and without supervision is enormous: there is a huge number of possible feature combinations, the number of which exponentially increases with each additional layer — thus an effective learning algorithm must be employed.

In this paper, the idea is to represent the objects with a *learned hierarchical compositional shape vocabulary* that has the following architecture. The vocabulary at each layer contains a set of hierarchical deformable models which we will call *compositions*. Each composition is defined recursively: it is a hierarchical *generative* probabilistic model that represents a geometric configuration of a small number of parts which are themselves hierarchical deformable models, i.e., compositions from a previous layer of the vocabulary. We present a framework for *learning* such a representation for multiple object classes. Learning is statistical and is performed bottom-up. The approach takes simple oriented contour fragments and learns their frequent spatial configurations. These are recursively combined into increasingly more complex and class-specific shape compositions, each exerting a high degree of shape variability. In the top-level of the vocabulary, the compositions are sufficiently large and complex to represent the whole shapes of the objects. We learn the vocabulary layer after layer, by gradually increasing the size of the window of analysis and the spatial resolution at which the shape configurations are learned. The lower layers are learned jointly on images of all classes, whereas the higher layers of the vocabulary are learned incrementally, by presenting the algorithm with one object class after another. We assume supervision in terms of a positive and a validation set of class images — however, the structure of the vocabulary is learned in an *unsupervised* manner. That is, the number of compositions at each layer, the number of parts for each of the compositions along with the distribution parameters are inferred from the data without supervision.

We experimentally demonstrate several important issues: **1.)** Applied to a collection of natural images, the approach *learns* hierarchical models for various curvatures, T- and L- junctions, i.e., features usually emphasized by the Gestalt theory [23]; **2.)** We show that these generic compositions can be effectively used for object classification; **3.)** For object detection we demonstrate a competitive speed of detection with respect to the related approaches already for a single class. **4.)** For multi-class object detection we achieve a highly sub-linear growth in the size of the hierarchical vocabulary at multiple layers and, consequently, a scalable complexity of inference as the number of modeled classes increases; **5.)** We demonstrate a competitive detection accuracy with respect to the current state-of-the-art. Furthermore, the learned representation is very compact — a hierarchy modeling 15 object classes uses only 1.6Mb on disk.

The remainder of this paper is organized as follows.

In Sec. 2 we review the related work. Sec. 3 presents our hierarchical compositional representation of object shape with recognition and detection described in Sec. 4. In Sec. 5 our learning framework is proposed. The experimental results are presented in Sec. 6. The paper concludes with a summary and discussion in Sec. 7 and pointers to future work in Sec. 8.

## 2 RELATED WORK AND CONTRIBUTIONS

**Compositional hierarchies.** Several compositional approaches to modeling objects have been proposed in the literature, however, most of them relied on hand-crafted representations, pre-determined grouping rules or supervised training with manually annotated object parts [10], [19], [20], [24]. The reader is referred to [10], [25] for a thorough review.

**Unsupervised learning of hierarchical compositional vocabularies.** Work on *unsupervised hierarchical learning* has been relatively scarce. Utans [26] has been the first to address unsupervised learning of compositional representations. The approach learned hierarchical mixture models of feature combinations, and was utilized on learning simple dot patterns.

Based on the Fukushima’s model [27], Riesenhuber and Poggio [28] introduced the HMAX approach which represents objects with a 2-layer hierarchy of Gabor feature combinations. The original HMAX used a vocabulary of pre-determined features, while these have subsequently been replaced with randomly chosen templates [29]. Since no statistical learning is involved, as much as several thousands of features are needed to represent the objects. An improved learning algorithm has recently been proposed by Masquelier and Thorpe [30].

Among the neural network representatives, Convolutional nets [31], [32] have been most widely and successfully applied to generic object recognition. The approach builds a hierarchical feature extraction and classification system with fast feed-forward processing. The hierarchy stacks one or several feature extraction stages, each of which consists of filter bank layer, non-linear transformation layers, and a pooling layer that combines filter responses over local neighborhoods using an average or max operation, thereby achieving invariance to small distortions [32]. A similar approach is proposed by Hinton [33] with recent improvements by Ng et al. [34]. One of the main drawbacks of these approaches, however, may be that they do not explicitly model the spatial relations among the features and are thus potentially less robust to shape variations.

Bouchard and Triggs [7] proposed a 3–layer hierarchy (extension of the constellation model [1]) and a similar representation was proposed by Torralba et al. [2], [35]. For tractability, all of these models are forced to use very sparse image information, where prior to learning and detection, a small number (around 30) of interest points are detected. Using highly discriminative SIFT features might limit their success in cluttered images or

on structurally simpler objects with little texture. The repeatability of the SIFT features across the classes is also questionable [29]. On the other hand, our approach is capable of dealing with several tens of thousands of contour fragments as input. We believe that the use of repeatable, dense and indistinctive contour fragments provide us with a higher repeatability of the subsequent object representation facilitating a better performance.

Epshtein and Ullman [36] approached the representation from the opposite end; the hierarchy is built by *decomposing* object relevant image patches into recursively smaller entities. The approach has been utilized on learning each class individually while a joint multi-class representation has not been pursued. A similar line of work was adopted by Mikolajczyk et al. [37] and applied to recognize and detect multiple (5) object classes.

Todorovic and Ahuja [38] proposed a data-driven approach where a hierarchy for each object example is generated automatically by a segmentation algorithm. The largest repeatable subgraphs are learned to represent the objects. Since bottom-up processes are usually unstable, exhaustive grouping is employed which results in long training and inference times.

Ommer and Buhmann [12] proposed an unsupervised hierarchical learning approach, which has been successfully utilized for object classification. The features at each layer are defined as histograms over a larger, spatially constrained area. Our approach explicitly models the spatial relations among the features, which should allow for a more reliable detection of objects with lower sensitivity to background clutter.

The learning frameworks most related to ours include the work by [39], [40] and just recently [41]. However, all of these methods build *separate* hierarchies for each object class. This, on the one hand, avoids the massive number of possible feature combinations present in diverse objects, but, on the downside, does not exploit the shareability of features among the classes.

Our approach is also related to the work on multi-class shape recognition by Amit et al. [42], [43], [15], and some of their ideas have also inspired our approach. While the conceptual representation is similar to ours, the compositions there are designed by hand, the hierarchy has only three layers (edges, parts and objects), and the application is mostly targeted to reading licence plates.

While surely equally important, the work on learning of visual taxonomies [44], [45] of object classes tackles the categorization/recognition process by hierarchical cascade of classifiers. Our hierarchy is compositional and generative with respect to object structure and does not address the taxonomic organization of object classes. We proposed a model that is hierarchical both in structure as well as classes (taxonomy) in our later work [46].

Our approach is also related to the discriminatively trained grammars by Girshick et al. [13], developed after our original work was published. Like us, this approach models objects with deformable parts and subparts, the weights of which are trained using structure prediction.

This approach has achieved impressive results for object detection in the past years. Its main drawback, however, is that the structure of the grammar needs to be specified by hand which is what we want to avoid doing here.

Compositional representations are currently not at the level of performance of supervised deep convolutional networks [47] which discriminatively train millions of weights (roughly three orders of magnitude more weights than our approach). To perform well these networks typically need millions of training examples, which is three or four orders of magnitude more than our approach. While originally designed for classification these networks have recently been very successful in object detection when combined with bottom-up region proposals [48]. We believe that these type of networks can also benefit from the ideas presented here.

**Contour-based recognition approaches.** Since our approach deals with object shape, we also briefly review the related work on contour-based object class detection.

Contour fragments have been employed in the earlier work by Selinger and Nelson [49] and a number of follow-up works have used a similar approach. Opelt et al. [3] learned *boundary fragments* in a boosting framework and used them in a Hough voting scheme for object class detection. Ferrari et al. [50], [5] extracted kPAS features which were learned by combining  $k$  roughly straight contour fragments. The learned kPAS features resemble those obtained in the lower hierarchical layers by our approach. Fergus et al. [51], [1] represent objects as constellations of object parts and propose an approach that learns the model from images without supervision and in a scale invariant manner. The part-based representation is similar to ours, however in contrast, our approach learns a hierarchical part-based representation.

To the best of our knowledge, we are the first to 1.) *learn* generic shape structures from images at multiple hierarchical layers and without supervision, which, interestingly, resemble those predicted by the Gestalt theory [23], 2.) learn a multi-class generative compositional representation in a bottom-up manner from simple contour fragments, 3.) demonstrate scalability of a hierarchical generative approach when the number of classes increases — in terms of the speed of inference, storage, and training times.

This article conjoins and extends several of our conference papers on learning of a hierarchical compositional vocabulary of object shape [52], [11], [53], [54]. Specifically, the original model has been reformulated and more details have been included which could not be given in the conference papers due to page constraints. Further, more classes have been used in the experiments, the approach has been tested on several standard recognition benchmarks and an analysis with respect to the computational behavior of the proposed approach has been carried out.

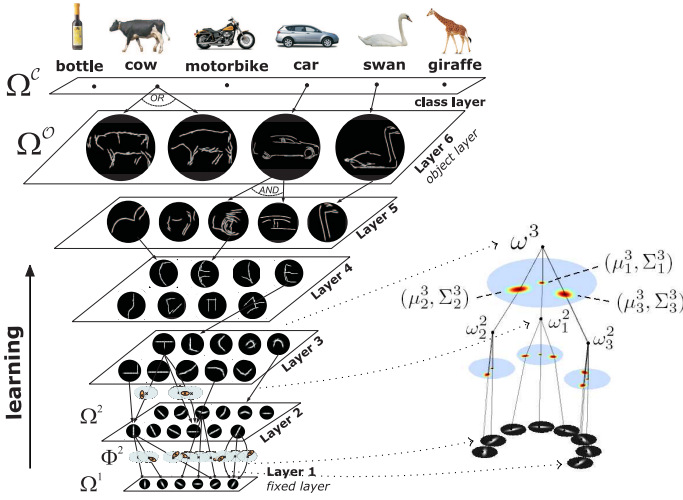


Fig. 1. **Left:** Illustration of the hierarchical vocabulary. The shapes depict the compositions  $\omega^\ell$  and the links between them denote the compositional relations between them. Note that there are no actual images stored in the vocabulary – the depicted shapes are *mean* shapes represented by the compositions. **Right:** An example of a complete composition model from layer 3. The blue patches are the limiting sizes within which the model can generate shapes, while the red ellipses denote the Gaussians representing the spatial relations between the parts.

### 3 A HIERARCHICAL COMPOSITIONAL OBJECT REPRESENTATION

The complete hierarchical framework addresses three major issues: the representation, inference and learning. In this Section we present our hierarchical compositional object representation.

Our aim is to model the distribution of object *shapes* in a given class and we wish to do so for multiple object classes in a computationally efficient way. The idea is to represent the objects with a *single learned hierarchical compositional shape vocabulary* that has the following architecture. The vocabulary at each layer contains a set of hierarchical deformable models which we will call *compositions*. Each composition is defined recursively: it represents a geometric configuration of a small number of parts which are compositions from the previous layer of the vocabulary. Different compositions can share models for the parts, which makes the vocabulary efficient in size and results in faster inference.

The geometric configuration of parts is modeled by relative spatial relations between each of the parts and one part called a *reference part*. The hierarchical “topology” of a composition is assumed to be a tree and is learned in a way to ensure that its (sub)parts do not overlap or overlap minimally.

Note that a particular shape can be composed in multiple different ways, e.g. a rectangle can be formed by two sets of parallel lines or four properly aligned right angles. Thus some of the compositions may describe the same shape but have very different topologies (different

tree structures). To deal with this issue, such compositions are grouped into OR nodes which act as mixture models (similarly as in [55]). This is done based on the geometric similarity of the shape they represent.

The structure of the compositions will be learned in an *unsupervised manner* from images, along with the corresponding parameters. The number of compositions that make a particular layer in the vocabulary will also not be set in advance but determined through learning. We will learn the layers 2 and 3 without any supervision, from a pool of unlabeled images. To learn the higher layers, we will assume bounding boxes with object labels, i.e., the set of positive and validation boxes of objects for each class needs to be given. The amount of supervision the approach needs is further discussed in Sec. 5.2.

At the lowest (first) layer, the hierarchical vocabulary consists of a small number of base models that represent short contour fragments at coarsely defined orientations. The number of orientations is assumed given. At the top-most layer the compositions will represent the shapes of the whole objects. For a particular object class, a number of top-layer compositions will be used to represent the whole distribution of shapes in the class, i.e., each top-layer composition will model a certain aspect (3D view or an articulation) of the objects within the class. The left side of Fig. 1 illustrates the representation.

Due to the recursive definition, a composition at any layer of the vocabulary is thus an “autonomous” deformable model. As such, a composition at the top layer can act as a detector for an object class, while a composition at an intermediate layer acts as a detector for a less complex shape (for example, an L junction). Since we are combining deformable models as we go up in the hierarchy, we are capturing an increasing variability into the representation while at the same time preserving the spatial arrangements of the shape components.

We will use the following notation. Let  $\Omega$  denote the set and structure of all compositions in the vocabulary and  $\Theta$  their parameters. Since the vocabulary has a hierarchical structure we will write it as  $\Omega = \Omega^1 \cup \Omega^1 \cup \Omega^2 \cup \Omega^2 \cup \dots \cup \Omega^O \cup \Omega^C$  where  $\Omega^\ell = \{\omega_i^\ell\}_i$  is a set of compositions at layer  $\ell$  and  $\bar{\Omega}^\ell = \{\bar{\omega}_i^\ell\}_i$  is a set of OR-compositions from layer  $\ell$ , more specifically,  $\bar{\omega}_i^\ell \subseteq \Omega^\ell$ . Whenever it is clear from the context, we will omit the index  $i$ . With  $\Omega^O$  we denote the top, *object layer* of compositions (we will use  $O = 6$  in this paper, and this choice is discussed in Sec. 5.2), which roughly code the whole shapes of the objects. The final, *class layer*  $\Omega^C$ , is an OR layer of object layer compositions ( $\Omega^O$ ), i.e., each class layer composition pools all of the corresponding object layer compositions from  $\Omega^O$  for each class separately.

The definition of a composition with respect to just one layer below is similar to that of the constellation model [51]. A *composition*  $\omega^\ell$ , where  $\ell > 1$ , consists of  $P$  parts ( $P$  can differ across compositions), with *appearances*  $\theta_a^\ell = [\theta_{a_j}^\ell]_{j=1}^P$  and *geometric parameters*  $\theta_g^\ell = [\theta_{g_j}^\ell]_{j=1}^P$ . The parts are compositions from the previous OR layer

$\bar{\Omega}^{\ell-1}$ . One of the parts that forms  $\omega^\ell$  is taken as a reference and the positions of other parts are defined relative to its position. We will refer to such a part as a *reference part*.

The appearance  $\theta_{aj}^\ell$  is an  $N^{\ell-1}$  dimensional vector, where  $N^{\ell-1} = |\bar{\Omega}^{\ell-1}|$  is the number of OR-compositions at layer  $\ell - 1$ , and  $\theta_{aj}^\ell(k)$  represents the *compatibility* between  $\bar{\omega}_k^{\ell-1}$  and  $j$ -th part of  $\omega^\ell$ . This vector will be sparse, thus only the non-zero entries need to be kept. For example, imagine composing an object model for the class *car*. A car can have many different shapes for the trunk or the front of the car. Thus a car detector should “fire” if any part that looks like any of the trunks is present in the rear location and any front part in the front location of the detector. We allow  $\theta_{aj}^\ell$  to have multiple positive entries only at the object level  $\bar{\Omega}^O$ , for other layers we consider  $\theta_{aj}^\ell$  to be non-zero only at one entry (in this case, equal to 1).

The geometric relations between the position of each of the parts relative to the reference part are modeled by two-dimensional Gaussians  $\theta_{gj}^\ell = (\mu_j^\ell, \Sigma_j^\ell)$ . For the convenience of notation later on, we will also represent the location of a reference part with respect to itself with a Gaussian having zero mean and small variance,  $\epsilon^2 \text{Id}$ .

We allow for a composition to also have “repulsive” parts. These are the parts that the composition cannot consist of. For example, a handle is a repulsive part for a cup since its presence indicates the class mug. We introduce the repulsive parts to deal with compositions that are supersets of one another.

The models at the first layer of the vocabulary are defined over the space of image features, which will in this paper be  $n$ -dimensional Gabor feature vectors (explained in Sec. 4.1).

Note that each composition can only model shapes within a limited spatial extent, that is, the window around a modeled shape is of limited size and the size is the same for all compositions at a particular layer  $\ell$  of the vocabulary. We will denote it with  $r^\ell$ . The size  $r^\ell$  increases with the level of hierarchy. Fig. 2 depicts the gradual increase in complexity and spatial scope of the compositions in the hierarchy.

## 4 RECOGNITION AND DETECTION

The model is best explained by first considering inference. Thus, let us for now assume that the representation is already known and we are only concerned with recognizing and detecting objects in a query image given our hierarchical vocabulary. How we learn the representation will be explained in Sec. 5.

Sec. 4.1 explains the image features we use, which form a set of observations, and how we extract them from an image. Sec. 4.2 describes the inference of the hidden states of the model, while Sec. 4.3 shows how to perform it in a computationally efficient way.

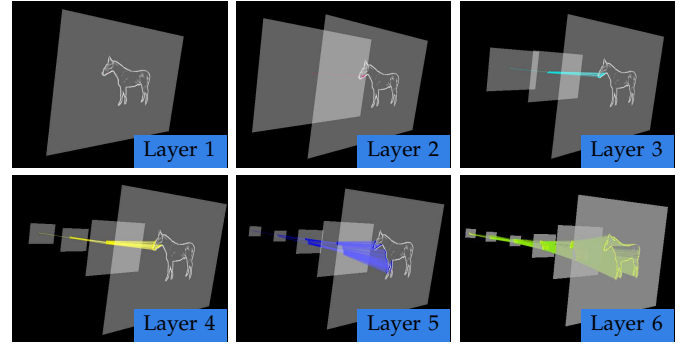


Fig. 2. Fig. shows inferred parse graphs (Sec. 4.2) for compositions from different layers of the hierarchy. The complexity and the size of shapes explained by the compositions gradually increases with the level of hierarchy.

### 4.1 Extracting image features

Let  $I$  denote a query image. The features which we extract from  $I$  should depend on how we define the base models at the first layer  $\Omega^1$  of the vocabulary. In this paper we choose to use oriented edge fragments, however, the learning and the recognition procedures are general and independent of this particular choice.

In order to detect oriented edges in an image we use a Gabor filter bank:

$$g_{\lambda, \varphi, \gamma, \sigma}(x, y, \psi) = e^{-\frac{u^2 + \gamma^2 v^2}{2\sigma^2}} \cos\left(\frac{2\pi u}{\lambda} + \varphi\right)$$

$$u = x \cos \psi - y \sin \psi, \quad v = x \sin \psi + y \cos \psi,$$

where  $(x, y)$  represents the center of the filter’s domain, and the parameters in this paper are set to  $(\lambda, \gamma, \sigma) = (6, 0.75, 2)$ . A set of two filter banks is used, one with even,  $\varphi = 0$ , and the other with odd,  $\varphi = -\frac{\pi}{2}$ , Gabor kernels defined for  $n$  equidistant orientations,  $\psi = i\frac{\pi}{n}$ ,  $i = 0, 1, \dots, n-1$ . For the experiments in this paper we use  $n = 6$ .

We convolve the image  $I$  with both filter banks and compute the total energy for each of the orientations [56]:

$$\mathcal{E}(x, y, \psi) = \sqrt{r_0^2(x, y, \psi) + r_{-\pi/2}^2(x, y, \psi)}, \quad (1)$$

where  $r_0(x, y, \psi)$  and  $r_{-\pi/2}(x, y, \psi)$  are the convolution outputs of even and odd Gabor filters at location  $(x, y)$  and orientation  $\psi$ , respectively. We normalize  $\mathcal{E}$  to have the highest value in the image equal to 1. We further perform a non-maxima suppression over the total energy  $\mathcal{E}$  to find the locations of the local maxima for each of the orientations. This is similar to performing the Canny operator and taking the locations of the binary responses. At each of these locations  $(x, y)$ , the set of which will be denoted with  $\mathbf{X}$ , we extract Gabor features  $\mathbf{f} = \mathbf{f}(x, y)$  which are  $n$ -dimensional vectors containing the orientation energy values in  $(x, y)$ ,  $\mathbf{f}(x, y) = [\mathcal{E}(x, y, i\frac{\pi}{n})]_{i=0}^{n-1}$ . Specifically, the feature set  $\mathbf{F}$  is the set of all feature vectors extracted in the image,  $\mathbf{F} = \{\mathbf{f}(x, y), (x, y) \in \mathbf{X}\}$ . The number of features in  $\mathbf{F}$  is usually around  $10^4$  for an image of average size and texture. The image features





Fig. 3. **Left:** Original image. **Middle:** Maximum over orientation energies,  $\arg \max_{\psi} \mathcal{E}(x, y, \psi)$ . **Right:** Points in which  $n$ -dimensional Gabor feature vectors  $\mathbf{f}$  are extracted. Different colors denote different dominant orientations of features  $\mathbf{f}$ .

$(\mathbf{F}, \mathbf{X})$  serve as the *observations* to the recognition procedure. Figure 3 shows an example of feature extraction.

*Scale.* The feature extraction as well as the recognition process is performed at several scales of an image: we use a Gaussian pyramid with two scales per octave and process each scale separately. That is, feature extraction and recognition up to the object level  $\mathcal{O}$  are performed at every scale and independently of other scales. For detection of object classes we then consider information from *all* scales. Not to overload the notation, we will just refer to one scale of  $I$ .

## 4.2 Inference

Performing inference in a query image with a given vocabulary entails inferring a hierarchy of hidden states from the observations (which are the image features  $(\mathbf{F}, \mathbf{X})$ ). The hidden states at the first layer will be the only ones receiving input directly from the observations, whereas all the other states will receive input from a hidden layer below.

Each hidden state  $z^\ell = (\omega^\ell, x^\ell)$  has two components:  $\omega^\ell$  denotes a composition from the vocabulary and  $x^\ell$  a location in an image (to abbreviate notation from here on, we will use  $x$  instead of  $(x, y)$  to denote the location vector). The notation  $x^\ell$  is used to emphasize that  $x$  is from a spatial grid with resolution corresponding to hidden layer  $\ell$ , i.e., the spatial resolution of the locations of the hidden states will be increasingly coarser with the level of hierarchy (discussed in Sec. 4.3).

To each hidden state  $z^\ell$  we associate its *score*,  $\text{score}(z^\ell)$ . The score captures the deformations and compatibility of the parts. It is recursively computed as follows:

$$\text{score}(z^\ell) = \prod_{p=1}^{P(\omega^\ell)} \max_{z_p^{\ell-1}} \left( \widehat{\text{score}}(z_p^{\ell-1}) \cdot D(x_j^{\ell-1} - x^\ell \mid \mu_j^\ell, \Sigma_j^\ell) \cdot \text{Comp}(\omega^\ell, \bar{\omega}_j^{\ell-1}, p) \right), \quad (2)$$

where, in general,  $\widehat{\text{score}}(z_p^{\ell-1}) := \text{score}(z_p^{\ell-1})$ , and  $D$  represents the deformation score function. We define it as an unnormalized Gaussian

$$D(x \mid \mu, \Sigma) = \exp \left( -0.5 \cdot (x - \mu)^T \Sigma^{-1} (x - \mu) \right) \quad (3)$$

Note that  $D$  is always from the interval  $[0, 1]$ , and is 1 when the part  $z^{\ell-1}$  is located at its expected relative

position  $\mu$ . The term  $\text{Comp}(\omega^\ell, \bar{\omega}_j^{\ell-1}, p)$  represents the compatibility between the  $p$ -th part of  $\omega^\ell$  and composition  $\bar{\omega}_j^{\ell-1}$ . We use  $\text{Comp}(\omega^\ell, \bar{\omega}_j^{\ell-1}, p) = \theta_{a_p}^\ell(j)$ . Our scores will always be from  $[0, 1]$ .

Note that a composition can also have repulsive parts. For these we take  $D$  to equal a constant  $\alpha$  (which we set to 0.1 in this paper) and we define  $\widehat{\text{score}}(z_p^{\ell-1}) := 1 - \text{score}(z_p^{\ell-1})$ . As an example, assume we have in our vocabulary a composition of three short horizontal edges as well as a composition of just two. The scoring function is set up in a way to prefer the larger composition if the image (local patch in the image) contains three strong horizontal edges while it will prefer the smaller composition if one of the edges is much weaker.

Score  $\text{score}(\bar{\omega}^\ell, x)$  of hidden state corresponding to an OR-composition is taken simply as maximum over all OR-ed compositions

$$\text{score}(\bar{\omega}^\ell, x) = \max_{\omega^\ell \in \bar{\omega}^\ell} \text{score}(\omega^\ell, x) \quad (4)$$

Due to recursive definition of the score and the fact that each composition is a tree we can use dynamic programming to compute the scores efficiently. Note however, that since the number of compositions in the vocabulary can be relatively large (order of hundreds), exhaustive computation would run too slow. We thus perform hypothesis pruning at each level and focus computation to only promising parts of the image. We explain this process in more detail in the next section.

## 4.3 Efficient computation

The process of inference in image  $I$  involves building an *inference graph*  $\mathcal{G} = \mathcal{G}_I = (Z, E)$  where the nodes  $Z$  of the graph are the (“promising”) hypotheses  $z^\ell$ . Graph  $\mathcal{G}$  has a hierarchical structure resembling that of the vocabulary, thus vertices  $Z$  are partitioned into vertex layers 1 to  $\mathcal{O}$ , that is,  $Z = Z^1 \cup \bar{Z}^1 \cup Z^2 \cup \bar{Z}^2 \dots \cup Z^\mathcal{O}$ . Vertices  $Z^\ell$  correspond to composition layer  $\Omega^\ell$  and vertices of  $\bar{Z}^\ell$  to OR layer  $\bar{\Omega}^\ell$ .

Assume that the hypotheses up to layer  $\ell - 1$ ,  $\bar{Z}^\ell$  have already been computed. To get the next layer we visit each hypothesis  $\bar{z}_i^{\ell-1}$ . For a particular  $\bar{z}_i^{\ell-1} = (\bar{\omega}_i^{\ell-1}, x^{\ell-1})$  we first *index* into the vocabulary to retrieve potential compositions  $\omega^\ell$  to be matched. As the candidate list we retrieve all  $\omega^\ell$  for which  $\bar{\omega}_i^{\ell-1}$  is one of its parts, i.e.  $\theta_{a_i}^\ell(i)$  is non-zero. This typically prunes the number of compositions to be matched significantly.

The matching process for a retrieved composition  $\omega^\ell$  entails computing the score defined in Eq. (2). If the hypothesis scores higher than a threshold  $\tau^\ell$  we add it to  $Z^{\ell-1}$ , otherwise we prune it. During the process of training (until the hierarchy is built up to the level of objects), these thresholds are fixed and set to very small values (in this paper we use  $\tau = 0.05$ ). Their only role is to prune the very unlikely hypotheses and thus both, speed-up computation as well as minimize the memory/storage requirements (the size of  $\mathcal{G}$ ). After the class models (the final, layer  $\Omega^\mathcal{O}$  of the vocabulary)

are learned we can also learn the thresholds in a way to optimize the speed of inference while retaining the detection accuracy, as will be explained in Sec. 5.2.1. Note that due to the thresholds, we can avoid some of the computation: we do not need to consider the spatial locations of parts that are outside the  $\tau^\ell$  Gaussian radius.

*Reduction in spatial resolution.* After each layer  $Z^\ell$  is built, we perform *spatial downsampling*, where the locations  $x^\ell$  of the hidden states  $z^\ell$  are downsampled by a factor  $\rho^\ell < 1$ . Among the states that code the same composition  $\omega^\ell$  and for which the locations (taken to have integer values) become equal, only the state with the highest score is kept. We use  $\rho^1 = 1$  and  $\rho^\ell = 0.5$ ,  $\ell > 1$ . This step is mainly meant to reduce the computational load: by reducing the spatial resolution at each layer, we bring the far-away (location-wise) hidden states closer. This, indirectly, keeps the scales of the Gaussians relatively small across all compositions in the vocabulary and makes inference faster.

The OR layer  $\bar{Z}^\ell$  pools all compositions  $z^\ell = (\omega^\ell, x^\ell) \in Z^\ell$  for which  $\{\bar{z}^\ell = (\bar{\omega}^\ell, x^\ell) : \omega^\ell \in \bar{\omega}^\ell\}$  into one node, which further reduces the hypotheses space.

Edges of  $\mathcal{G}$  connect vertices of  $Z^\ell$  to vertices of  $\bar{Z}^{\ell-1}$  and vertices of  $\bar{Z}^\ell$  to vertices of  $Z^\ell$ . Each  $z^\ell = (\omega^\ell, x^\ell)$  is connected to vertices  $\bar{z}_p^{\ell-1}$  that yield the max score for the part  $j$  in Eq. (2) and each vertex  $\bar{z}^\ell = (\bar{\omega}^\ell, x^\ell)$  connects to  $z^\ell$  giving the max value in Eq. (4). The subgraph of  $\mathcal{G}$  on vertices reachable from vertex  $z$  via downward edge paths is called a *parse graph* and denoted by  $\mathcal{P}(z)$ . A set of vertices of  $\mathcal{P}(z)$  from  $Z^1$ , i.e. layer 1 vertices reachable from  $z$  through edges in  $\mathcal{G}$ , are called *support* of  $z$  and denoted with  $\text{supp}(z)$ . See Fig. 2 for examples of parse graphs and supports of vertices from different layers. The definition of support is naturally extended to a set of nodes as  $\text{supp}(S) = \cup_{z \in S} \text{supp}(z)$ .

## 5 LEARNING

This section addresses the problem of learning the representation, which entails the following:

- 1) **Learning the vocabulary of compositions.** Finding an appropriate set of compositions to represent our data, learning the structure of compositions (the number of parts and a (rough) initialization of the parameters) and learning the OR-compositions.
- 2) **Learning the parameters of the representation.** Finding the parameters for spatial relations and appearance for each composition as well as the thresholds to be used in the approximate inference algorithm.

In the learning process our aim is to build a vocabulary of compositions which tries to meet the following two conditions: (a) Detections of compositions on the object layer,  $\Omega^\mathcal{O}$ , give good performance on the train/validation set. (b) The vocabulary is minimal, optimizing the inference time. Intuitively, it is possible to build a good composition on the object layer if the previous layer  $\Omega^{\mathcal{O}-1}$  produces a good “coverage” of training examples.

By coverage we mean that the supports of hypotheses in  $Z^{\mathcal{O}-1}$  contain most of the feature locations  $\mathbf{X}$ . Hence, we would like to build our vocabulary such that the compositions at each layer cover the feature location  $\mathbf{X}$  in the training set sufficiently well and is, according to (b), the most compact representation.

To find a good vocabulary according to the above constraints is a hard problem. Our strategy is to learn one layer at a time, in a bottom up fashion, and at each layer learn a small compact vocabulary while maintaining its good coverage ratio. Bottom-up layer learning is also the main strategy adopted to learn the convolutional networks [31], [33].

We emphasize that our learning algorithm uses several heuristics and is not guaranteed to find the optimal vocabulary. Deriving a more mathematically elegant learning approach is part of our future work.

### 5.1 Learning the structure

Here we explain how we learn the initial set of compositions, their structure and initial values of the parameters (which are re-estimated as described in Sec. 5.1.4).

The first layer,  $\ell = 1$ , is fixed thus the first layer that we learn is  $\ell = 2$ . Since learning the vocabulary is recursive we will describe how to learn layer  $\ell$  from  $\ell - 1$ . We will assume that for each training image  $I$  we have the inference graph  $\mathcal{G}_I = (Z, E)$  built up to layer  $\ell - 1$ , which is obtained as described in Sec. 4.2.

Define a spatial neighborhood of radius  $r^\ell$  around the node  $z^{\ell-1} = (\bar{\omega}^{\ell-1}, x^{\ell-1})$  with  $\mathcal{N}(z^{\ell-1})$ . We also define the *support* of  $\mathcal{N}(z^{\ell-1})$  by re-projecting the circular area to the original image resolution and finding all image features whose locations fall inside the projected circular area. Our goal in learning is to find a vocabulary that best explains all of the spatial neighborhoods  $\mathcal{N}(z^{\ell-1})$ , where  $z^{\ell-1} \in Z^{\ell-1}$ :

$$\Omega_*^\ell = \arg \max_{\Omega^\ell} \left( -C \sum_{\omega_i^\ell \in \Omega^\ell} P(\omega_i^\ell) + \sum_{I_j} \sum_{k \mid z_k^{\ell-1} \in Z_{I_j}^{\ell-1}} \text{score}(\mathcal{N}(z_k^{\ell-1}), \Omega^\ell) \right) \quad (5)$$

Here  $P(\omega_i^\ell)$  is the number of parts that defines a composition  $\omega_i^\ell$ , and  $C$  is a weight that balances the two terms. We define the score term as follows:

$$\text{score}(\mathcal{N}(z_k^{\ell-1}), \Omega^\ell) = \max_{z^\ell} \left( \text{score}_{\text{coverage}}(\mathcal{N}(z_k^{\ell-1}), z^\ell) + \text{score}_{\text{tree}}(z^\ell) \right), \quad (6)$$

where

$$\text{score}_{\text{coverage}}(\mathcal{N}(z_k^{\ell-1}), z^\ell) = \frac{|\text{supp}(z^\ell) \cap \text{supp}(\mathcal{N}(z_k^{\ell-1}))|}{|\text{supp}(z^\ell) \cup \text{supp}(\mathcal{N}(z_k^{\ell-1}))|} \quad (7)$$

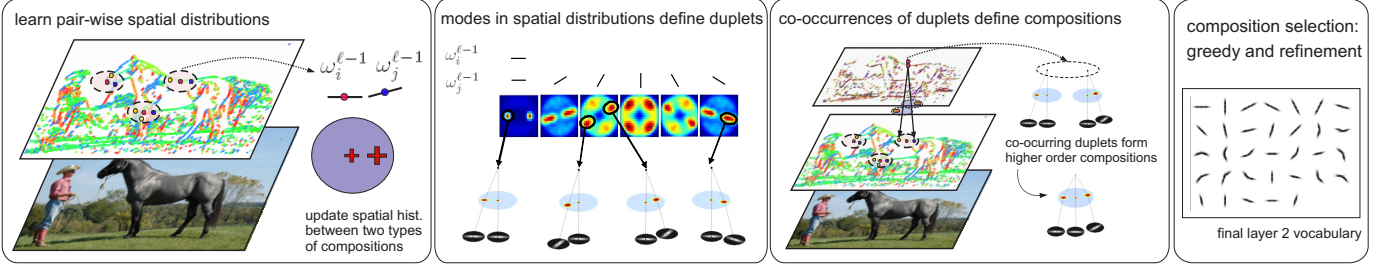


Fig. 4. Approach to learning the structure and the parameters of the vocabulary at a particular layer.

and

$$\text{score}_{\text{tree}}(z^\ell) = \begin{cases} -\infty & \text{if supports of any two pairs of} \\ & \text{parts of } z^\ell \text{ overlap more than 0.2} \\ 0 & \text{otherwise} \end{cases} \quad (8)$$

Our learning strategy will be the following:

- 1) First learn the relative spatial relations between all possible pairs of compositions from layer  $\ell - 1$ .
- 2) Detect the modes in these distributions which will define two-part compositions called *duplets*.
- 3) Find a set of all compositions, where each composition is a set of (frequently) co-occurring duplets that form a tree.
- 4) Select a subset of compositions that tries to optimize the scoring function (5).
- 5) Learn the OR layer by finding clusters of compositions that detect similar shapes.

The overall learning procedure is illustrated in Fig. 4.

### 5.1.1 Learning spatial correlations between parts

We start by learning the spatial relations among *pairs* of compositions  $(\bar{\omega}_i^{\ell-1}, \bar{\omega}_j^{\ell-1}) \in \bar{\Omega}^{\ell-1} \times \bar{\Omega}^{\ell-1}$ . The first composition  $\bar{\omega}_i^{\ell-1}$  in the pair plays the role of a *reference*. This means that the spatial relations will be learned relative to it. We will learn these relations by visiting all pairs of states in the inference graphs  $\bar{Z}^{\ell-1}$  that are within  $r^\ell$  distance of each other (the choice of  $r^\ell$  is described below). We learn the spatial relations by means of two-dimensional histograms  $h_{ij}$  of size  $[-r^\ell, r^\ell] \times [-r^\ell, r^\ell]$ .

During training, each histogram  $h_{ij}^\ell$  is updated at location  $x^{\ell-1} - x^{\ell-1}$  for each pair of hidden states  $(z^{\ell-1}, z'^{\ell-1})$ , where  $z^{\ell-1} = (\bar{\omega}_i^{\ell-1}, x^{\ell-1})$  and  $z'^{\ell-1} = (\bar{\omega}_j^{\ell-1}, x'^{\ell-1})$ , satisfying:

- 1)  $|x^{\ell-1} - x'^{\ell-1}| \leq r^\ell$ , that is,  $z'^{\ell-1}$  lies in the circular area around  $z$  with radius  $r^\ell$ .
- 2)  $z^{\ell-1}$  and  $z'^{\ell-1}$  have disjoint supports. We enforce this to ensure that the resulting composition will have a tree topology, i.e. parts in each composition do not overlap spatially (or overlap minimally). The overlap of the supports is calculated as:

$$o(z^{\ell-1}, z'^{\ell-1}) = \frac{|\text{supp}(z^{\ell-1}) \cap \text{supp}(z'^{\ell-1})|}{|\text{supp}(z^{\ell-1}) \cup \text{supp}(z'^{\ell-1})|}$$

We allow for a small overlap of the parts, i.e., we select  $(z^{\ell-1}, z'^{\ell-1})$  for which  $o(z^{\ell-1}, z'^{\ell-1}) < 0.2$ .

The histograms are updated for all graphs  $\mathcal{G}_I$  and all the admissible pairs of hypotheses at layer  $\bar{Z}^{\ell-1}$ .

*The choice of  $r^\ell$ .* The correlation between the relative positions of the hypotheses is the highest at relatively small distances as depicted in Fig. 6. In this paper we set the radii  $r^\ell$  to 8 for layer 2, 12 for the higher layers, and 15 for the final, object layer, but this choice in general depends on the factors of the spatial downsampling (described in Sec. 4.3). Note that the circular regions are defined at spatial resolution of layer  $\ell - 1$  which means that the area, if projected back to the original resolution (taking into account the downsampling factors), covers a much larger area in an image.

*Finding the initial vocabulary: duplets.* From the computed pair-wise histograms we form *duplets* by finding the modes of the spatial distributions. Fig. 5 illustrates the clustering procedure. For each mode we estimate the mean  $\mu^\ell$  and variance  $\Sigma^\ell$  by fitting a Gaussian distribution around it. Each of these modes thus results in a two-part composition with initial parameters:  $P = 2$ ,  $\theta_{a1}^\ell(\omega_i^\ell) = 1$ ,  $\theta_{a2}^\ell(\omega_j^\ell) = 1$  and  $\theta_{g2}^\ell = (\mu^\ell, \Sigma^\ell)$  (the first, reference part, in a composition is always assigned the default parameters as explained in Sec. 3). For the higher layers,  $\ell > 3$ , where the co-occurrences are sparser, we additionally smooth the histograms prior to clustering, to regularize the data.

### 5.1.2 From duplets to compositions

Once we have the duplets our goal is to combine them into possibly higher-order (multi-part) *compositions*. We can form a composition whenever two or more different duplets share the same part. For example, we can combine a duplet defined by  $\theta_{a1}^\ell(i) = 1$ ,  $\theta_{a2}^\ell(j) = 1$  and  $\theta_{g2}^\ell = (\mu_1^\ell, \Sigma_1^\ell)$ , and a duplet defined by  $\theta_{a1}^\ell(i) = 1$ ,  $\theta_{a2}^\ell(k) = 1$  and  $\theta_{g2}^\ell = (\mu_2^\ell, \Sigma_2^\ell)$ , into a composition with  $P = 3$ ,  $\theta_{a1}^\ell(i) = 1$ ,  $\theta_{a2}^\ell(j) = 1$ ,  $\theta_{a3}^\ell(k) = 1$ , and  $\theta_{g2}^\ell = (\mu_1^\ell, \Sigma_1^\ell)$ ,  $\theta_{g3}^\ell = (\mu_2^\ell, \Sigma_2^\ell)$ . We will also allow a composition to only consist of a single duplet. We have a very loose restriction on the upper bound of the number of parts, i.e., we do not consider compositions of more than  $P = 10$  parts. We find the compositions by matching the duplets to each of the neighborhoods and keeping count of co-occurring duplets. Since each duplet is defined as one part spatially related to another, reference, part, we will only count co-occurrences whenever two or more



duplets share the same reference part (state  $z_1^{\ell-1}$  in this case). We next describe this procedure in more detail.

We first perform inference with our vocabulary of duplets. We match the duplets in each neighborhood  $\mathcal{N}(z_k^{\ell-1})$  by restricting that the matched reference part for each duplex to be  $z_k^{\ell-1}$  and match the other part of the duplex to the remaining states whose locations fall inside  $\mathcal{N}(z_k^{\ell-1})$ . We keep all matches for which the score computed as in Eq.(2) is above a threshold  $\tau^\ell$ . Denote a duplex match with  $\hat{z}_j^\ell$  which has parts  $z_k^{\ell-1} = (\bar{\omega}_k^{\ell-1}, x_k^{\ell-1})$  and  $z_j^{\ell-1} = (\bar{\omega}_j^{\ell-1}, x_j^{\ell-1})$ .

For each  $\mathcal{N}(z_k^{\ell-1})$  we then find all subsets  $z_j^\ell = \{\hat{z}_{j_p}^\ell\}_{p=1}^P$  of matched duplets which form trees, i.e., overlap (measured as intersection over union) of supports between each pair  $(z_{j_p}^{\ell-1}, z_{j_q}^{\ell-1})$  in the subset is lower than a threshold (0.2). Note that the reference part  $z_k^{\ell-1}$  is common to all duplex match matches (due to our restriction) and thus we are only checking the overlaps between the second parts of duplets in  $z_j^\ell$ . We compute  $\text{score}_{\text{coverage}}(\mathcal{N}(z_k^{\ell-1}), z_j^\ell)$  for each  $z_j^\ell$  as defined in Eq. (7).

Each  $z_j^\ell = \{\hat{z}_{j_p}^\ell\}_{p=1}^P$  defines a higher-order composition  $\omega_j^\ell$  with  $P+1$  parts,  $\theta_{a_1}^\ell(k) = 1$ ,  $\{\theta_{a_{p+1}}^\ell(j_p) = 1\}_{p=1}^P$ ,  $\{\theta_{g_{p+1}}^\ell = (\mu_{j_p}^\ell, \Sigma_{j_p}^\ell)\}_{p=1}^P$ . We do not make a difference between different permutations of parts thus we always order  $\{\omega_{j_p}\}$  by increasing index values.

We take a pass over all neighborhoods  $\mathcal{N}(z_k^{\ell-1})$  in all training images and keep track of all different  $\omega_j^\ell$  and update their score values. Note that some combinations of duplets will never occur, and is thus better to keep a sorted list of all  $\omega_j^\ell$  that occur at least once, and add to it if a new combination appears. Denote with  $\bar{\Omega}_0^\ell$  the large set of compositions obtained in this step. In the next Subsec. we discuss how we select our vocabulary  $\Omega^\ell$  from this large pool of compositions.

### 5.1.3 Composition selection

The final vocabulary at layer  $\ell$  is formed using a two-stage procedure. We first use a simple greedy selection: the composition  $\omega_j^\ell$  with the highest score (minus  $C$  times its number of parts) is added to  $\Omega^\ell$  first. We next visit all neighborhoods  $\mathcal{N}(z_k^{\ell-1})$  for which  $\omega_j^\ell$  was among the tree matches, and recompute the scores of all other matching tree compositions  $z_{j'}^\ell$ , as  $\text{score}'_{\text{coverage}}(\mathcal{N}(z_k^{\ell-1}), z_{j'}^\ell) = \text{score}_{\text{coverage}}(\mathcal{N}(z_k^{\ell-1}), z_{j'}^\ell) - \text{score}_{\text{coverage}}(\mathcal{N}(z_k^{\ell-1}), z_j^\ell)$ . We remove all  $z_{j'}^\ell$  for which the new score is lower than  $\epsilon$ . We use the  $\epsilon$  slack for efficiency – the larger our current vocabulary is the less neighborhoods we need to update. We again select the composition with the highest new score and repeat the procedure. We stop when the highest score is lower than a threshold (set empirically).

We next employ a stochastic MCMC algorithm to get the final vocabulary at layer  $\ell$ ,  $\Omega^\ell$ . The first state of the Markov chain is the vocabulary  $\Omega_g^\ell$  obtained with the greedy selection. Let  $\Omega_t^\ell$  denote the vocabulary at the current state of the chain. At each step we either exchange/add/remove one composition from  $\Omega_t^\ell$  with

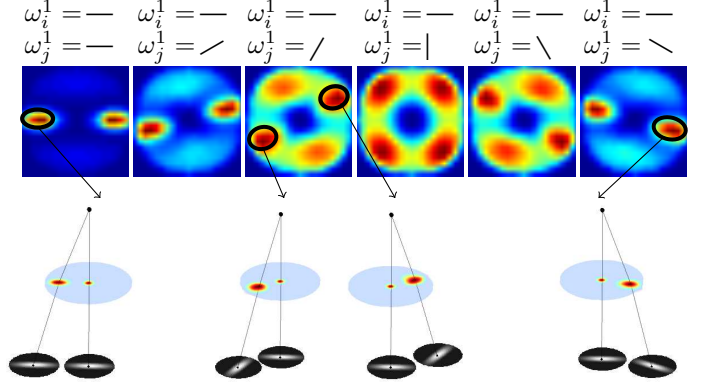


Fig. 5. **Top:** Examples of histograms  $h_{ij}^{\ell=2}$ . **Bottom:** Examples of duplets defined by modes in  $h_{ij}^{\ell=2}$ . The number of all duplets here would be 2 for the first two and the last histogram, and 4 for the third, fourth and fifth histogram, with the total of 18 duplets.

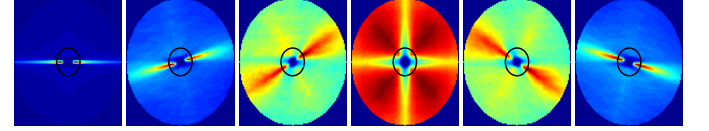


Fig. 6. Examples of learned histograms  $h_{ij}^{\ell=2}$  for very large radius,  $r^\ell = 50$ . The circle shows the chosen radius,  $r^\ell = 8$ .

another one from  $\Omega_0^\ell \setminus \Omega_t^\ell$  to get the vocabulary  $\Omega_{t+1}^\ell$ . The vocabulary  $\Omega_{t+1}^\ell$  is accepted as the next state of the Markov chain with probability

$$\min(1, \beta^{\text{score}(\Omega_t^\ell) - \text{score}(\Omega_{t+1}^\ell)}), \quad \beta > 1 \quad (9)$$

according to the Metropolis-Hastings algorithm.

The vocabulary at layer  $\ell$  is finally defined as the  $\Omega^\ell$  with maximal value of  $\text{score}(\Omega^\ell)$ , after running several iterations of the M-H algorithm. We usually perform 100 iterations. This vocabulary refinement step has shown to slightly improve results [52].

To train the top, object-layer of compositions, we make use of the available supervision, similarly as in the constellation model [57]. During the greedy selection of the compositions, we always select the one with the highest detection accuracy (we use the F-measure).

### 5.1.4 (Re-)Estimating the parameters

Subsec. 5.1.3 yields a vocabulary at layer  $\ell$ . However, notice that the parameters (spatial relations) have been inherited from the duplets and thus may not be optimal for each full composition. We thus make several EM-like iterations through the data to adjust the parameters: We first hold the current parameters fixed and do inference on all neighborhoods in all images. For each neighborhood we take the best scoring composition whose matching score is higher than  $\tau^\ell$ . For each such detection we store the locations of the parts. For each composition type we then re-estimate the Gaussian distributions using the locations of parts from all detections.

For the top, object layer we also update the appearance parameters  $\theta_a^{\mathcal{O}}$  for each composition. We do this via co-occurrence in the following way. Suppose  $z^\ell = (\omega^\ell, x^\ell)$  is our top scoring composition for neighborhood  $\mathcal{N}$ , and  $z_p^{\ell-1}$  is the best match for the  $p$ -th part. We then find all states  $z_q^{\ell-1} = (\bar{\omega}_q^{\ell-1}, x_q^{\ell-1})$  for which the IOU overlap of the supports  $\text{supp}(z_p^{\ell-1})$  and  $\text{supp}(z_q^{\ell-1})$  exceeds 0.8. We update a histogram  $\bar{\theta}_a^{\ell}(q)$ . We take a pass through all neighborhoods, and finally normalize the histogram to obtain the final appearance parameters.

We only still need to infer the parameters for the first layer models in the vocabulary. This is done by estimating the parameters  $(\mu_i^1, \Sigma_i^1)$  of a multivariate Gaussian distribution for each model  $\omega_i^1$ : Each Gabor feature vector  $\mathbf{f}$  is first normalized to have the dominant orientation equal to 1. All features  $\mathbf{f}$  that have the  $i$ -th dimension equal to 1 are then used as the training examples for estimating the parameters  $(\mu_i^1, \Sigma_i^1)$ .

### 5.1.5 Getting the OR layers

Different compositions can have different tree structures but can describe approximately the same shape. We want to form OR nodes (disjunctions or mixtures) of such compositions. We do this by running inference with our vocabulary and selecting a number of different detections for each composition  $\omega^\ell$ . For each detection  $z^\ell = (\omega^\ell, x^\ell)$  we compute the Shape Context descriptor [58] on the support  $\text{supp}(z^\ell)$ . For each  $\omega^\ell$  we compute a prototype descriptor, one that is most similar to all other descriptors using the  $\chi^2$  similarity measure. We perform agglomerative clustering on the prototypical descriptors which gives us the clusters of compositions. Each cluster defines an OR node at layer  $\Omega^\ell$ .

## 5.2 Learning a multi-class vocabulary

In order to learn a single vocabulary to represent multiple object classes we use the following strategy. We learn layers 2 and 3 on a set of natural images containing scenes and objects without annotations. This typically results in very generic vocabularies with compositions shared by many classes. To learn layer 4 and higher we use annotations in the form of bounding boxes with class labels. We learn the layers incrementally, first using only images of one class, and then incrementally adding the compositions to the vocabulary on new classes.

When training the higher layers we scale each image such that the diagonal of the bounding box is approximately 250 pixels, and only learn our vocabulary within the boxes. Note that the size of the training images has a direct influence on the number of layers being learned (due to compositionality, the number of layers needed to represent the whole shapes of the objects is logarithmic in the number of extracted edge features in the image). In order to learn a 6-layer hierarchy, the 250 pixel diagonal constraint has proven to be a good choice.

Once we have learned the multi-class vocabulary, we could, in principle, run the parameter learning algorithm

(Sec. 5.1.4) to re-learn the parameters over the complete hierarchy in a similar fashion as in the Hierarchical HMMs [59]. However, we have not done so in this paper.

### 5.2.1 Learning the thresholds for the tests

Given that the object class representation is known, we can learn the thresholds  $\tau_{\omega^\ell}$  to be used in our (approximate) inference algorithm (Sec. 4.3).

We use a similar idea to that of Amit et al. [42] and Fleuret and Geman [40]. The main goal is to learn the thresholds in way that nothing is lost with respect to the accuracy of detection, while at the same time optimizing for the efficiency of inference.

Specifically, by running the inference algorithm on the set of class training images  $\{I_k\}$ , we obtain the object detection scores  $\text{score}(z^{\mathcal{O}})$ . For each composition  $\omega^\ell$  we find the smallest score it produces in any of the parse graphs of positive object detections  $z^{\mathcal{O}}$  over all train images  $I_k$ . Threshold for its score is then:

$$\tau_{\omega^\ell} = \min_k \min_{(\omega^\ell, x) \in \mathcal{P}_{I_k}(z^{\mathcal{O}})} \text{score}(\omega^\ell, x). \quad (10)$$

For a better generalization, however, one can rather take a certain percentage of the value on the right [40].

## 6 EXPERIMENTAL RESULTS

The evaluation is separated into two parts. We first show the capability of our method to learn generic shape structures from natural images and apply them to a object classification task. Second, we utilize the approach for multi-class object detection on 15 object classes.

All experiments were performed on one core on a Intel Xeon-4 CPU 2.66 Ghz computer. The method is implemented in C++. Filtering is performed on CUDA.

### 6.1 Natural statistics and object classification

We applied our learning approach to a collection of 1500 natural images. Learning was performed only up to layer 3, with the complete learning process taking roughly 5 hours. The learned hierarchy consisted of 160 compositions on Layer 2 and 553 compositions on Layer 3. A few examples from both layers are depicted in Fig. 8 (note that the images shown are only the mean shapes modeled by the compositions). The learned features include corners, end-stopped lines, various curvatures, T- and L-junctions. Interestingly, these structures resemble the ones predicted by the Gestalt rules [23].

To put the proposed hierarchical framework in relation to other categorization approaches which focus primarily shape, the learned 3-layer vocabulary was tested on the Caltech-101 database [60]. The Caltech-101 dataset contains images of 101 different object categories with the additional background category. The number of images varies from 31 to 800 per category, with the average image size of roughly  $300 \times 300$  pixels.

Each image was processed at 3 scales spaced apart by  $\sqrt{2}$ . The scores of the hidden states were combined

with a linear one-versus-all SVM classifier [61]. This was done as follows: for each image a vector of a dimension equal to the number of compositions at the particular layer was formed. Each dimension of the vector, which corresponds to a particular type of a composition (e.g. an L-junction) was obtained by summing over all scores of the hidden states coding this particular type of composition. To increase the discriminative information, a radial sampling was used similarly as in [62]: each image was split into 5 orientation bins and 2 distances from the image center, for which separate vectors (as described previously) were formed and consequently stacked together into one, high-dimensional vector.

The results, averaged over 8 random splits of train and test images, are reported in Table 1 with classification rates of existing hierarchical approaches shown for comparison. For 15 and 30 training images we obtained a 60.5% and 66.5% accuracy, respectively, which is slightly better than the most related hierarchical approaches [12], [63], [32], comparable to those using more sophisticated discriminative methods [64], [65], and slightly worse than those using additional information such as color or regions [66].

We further tested the classification performance by varying the number of training examples. For testing, 50 examples were used for the classes where this was possible and less otherwise. The classification rate was normalized accordingly. In all cases, the result was averaged over 8 random splits of the data. The results are presented and compared with existing methods in Fig. 7. We only compare to approaches that use shape information alone and not also color and texture. Overall, better performance has been obtained in [67].

TABLE 1  
Average classification rate (in %) on Caltech 101.

	$N_{train} = 15$	$N_{train} = 30$
Mutch et al. [63]	51	56
Ommer et al. [12]	/	61.3
Ahmed et al. [65]	58.1	67.2
Yu et al. [64]	59.2	<b>67.4</b>
Lee et al. [34]	57.7	65.4
Jarrett et al. [32]	/	65.5
<b>our approach</b>	<b>60.5</b>	66.5

## 6.2 Object class detection

The approach was tested on 15 diverse object classes from standard recognition datasets. The basic information is given in Table 2. These datasets are known to be challenging because they contain a high amount of clutter, multiple objects per image, large scale differences of objects and exhibit a significant intra class variability.

For training we used the bounding box information of objects or the masks if they were available. Each object was resized so that its diagonal in an image was approximately 250 pixels. For testing, we up-scaled each test image by a factor 3 and used 6 scales for object detection. When evaluating the detection performance, a

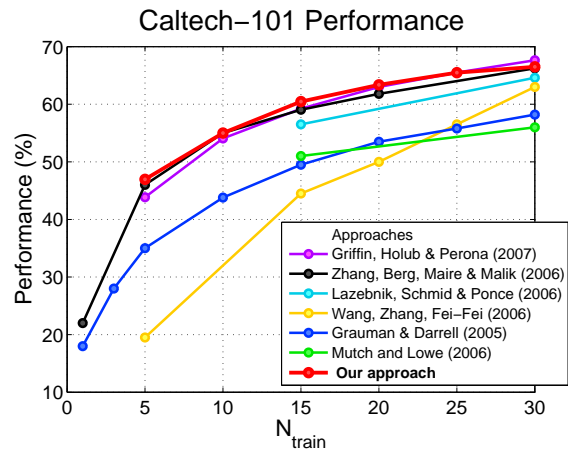


Fig. 7. Classification performance on Caltech-101.

detection is counted as correct, if the predicted bounding box  $b_{fg}$  coincides with the ground truth  $b_{gt}$  more than 50%:  $\frac{area(b_{fg} \cap b_{gt})}{area(b_{fg} \cup b_{gt})} > 0.5$ . On the ETH dataset and INRIA horses this threshold is lowered to 0.3 to enable a fair comparison with the related work [50]. The performance is given either with recall at equal error rate (EER) or positive detection rate at low FPPI, depending on the type of results reported on these datasets thus-far.

### 6.2.1 Single class learning and performance

We first evaluated our approach to learn and detect each object class individually. We report the training and inference times, and the accuracy of detection, which will then be compared to the multi-class case in Sec. 6.2.2 to test the scalability of the approach.

*Training time.* To train a class it takes on average 20–25 minutes. For example, it takes 23 minutes to train on Apple logo, 31 for giraffe, 17 for swan, 25 for cow, and 35 for the horse class. For comparison, in Shotton et al. [4], training on 50 horses takes roughly 2 hours (on a 2.2 GHz machine using a C# implementation).

*Inference time.* Detection for each individual class takes from 2 – 4 seconds per image, depending on the size of the image and the amount of texture it contains. Other related approaches report approx. 5 to 10 times higher times (in seconds): [38]: 20 – 30, [41]: 16.9, [68]: 20, [1]: 12 – 18, however, at slightly older hardware.

*Detection performance.* The ETH experiments are performed in a 5-fold cross-validation obtained by sampling 5 subsets of half of the class images at random. The test set for evaluating detection consists of all the remaining images in the dataset. The detection performance is given as the detection rate at the rate of 0.4 false-positives per image (FPPI), averaged over the 5 trials as in [50]. The detection performance is reported in Table 3. Similarly, the results for the INRIA horses are given in a 5-fold cross-validation obtained by sampling 5 subsets of 50 class images at random and using the remaining 120 for testing. The test set also includes 170 negative images to allow for a higher FPPI rate. With respect to [50], we achieve a better performance for all classes, most notably

for giraffes (24.7%). Our method performs comparably to a discriminative framework by Fritz and Schiele [68]. Better performances have recently been obtained by Maji and Malik [69] (93.2%) and Ommer and Malik [70] (88.8%) using Hough voting and SVM-based verification. To the best of our knowledge, no other hierarchical approach has been tested on this dataset so far.

For the experiments on the rest of the datasets we report the recall at EER. The results are given in Table 3. Our approach achieves competitive detection rates with respect to the state-of-the-art. Note also that [37], [6] used 150 training examples of motorbikes, while we only used 50 (to enable a fair comparison with [3] on GRAZ).

While the performance in a single-class case is comparable to the current state-of-the-art, the main advantage of our approach are its computational properties when the number of classes is higher, as demonstrated next.

### 6.2.2 Multi-class learning and performance

To evaluate the scaling behavior of our approach we have incrementally learned 15 classes one after another.

*The learned vocabulary.* A few examples of the learned shapes at layers 4 to 6 are shown in Fig.9 (only samples from the generative model are depicted). An example of a complete object-layer composition is depicted in Fig. 13. It can be seen that the approach has learned the essential structure of the class well, not missing any important shape information.

*Degree of composition sharing among classes.* To see how shared are the vocabulary compositions between classes of different degrees of similarity, we depict the learned vocabularies for two visually similar classes (motorbike and bicycle), two semi-similar classes (giraffe and horse), and two dissimilar classes (swan and car\_front) in Fig. 10. The nodes correspond to compositions and the links denote the compositional relations between them and their parts. The green nodes represent the compositions used by both classes, while the specific colors denote class specific compositions. If a spatial relation is shared as well, the edge is also colored green. The computational advantage of our hierarchical representation over flat ones [3], [6], [2] is that the compositions are shared at *several* layers of the vocabulary, which significantly reduces the overall complexity of inference. Even for the visually dissimilar classes, which may not have any complex parts in common, our representation is highly shared at the lower layers of the hierarchy.

To evaluate the shareability of the learned compositions among the classes, we use the following measure:

$$\text{deg\_share}(\ell) = \frac{1}{|\bar{\Omega}^\ell|} \sum_{\bar{\omega}^\ell \in \bar{\Omega}^\ell} \frac{(\# \text{ of classes that use } \bar{\omega}^\ell) - 1}{\# \text{ of all classes} - 1},$$

defined for each layer  $\ell$  separately. By “ $\bar{\omega}^\ell$  used by class  $c$ ” it is meant that the probability of  $\bar{\omega}^\ell$  under  $c$  is not equal to zero. To give some intuition behind the measure:  $\text{deg\_share} = 0$  if no composition from layer  $\ell$  is shared (each class uses its own set of compositions), and it is 1

if each composition is used by all the classes. Fig. 12 (b) plots the values for the learned 15-class representation. Beside the mean (which defines *deg\_share*), the plots also show the standard deviation.

*The size of the vocabulary.* It is important to test how the size of the vocabulary (the number of compositions at each layer) scales with the number of classes, since this has a direct influence on inference time. We report the size as a function of the number of learned classes in Fig. 11. For the “worst case” we take the independent training approach: a vocabulary for each class is learned independently of other classes and we sum over the sizes of these separate vocabularies. One can observe a logarithmic tendency especially at the lower layers. This is particularly important because the complexity of inference is much higher for these layers (because they contain less discriminative compositions which are detected more numerous in images). Although the fifth layer contains highly class specific compositions, one can still observe a logarithmic increase in size. The final, object layer, is naturally linear in the number of classes, but it does, however, learn less object models than is the number of all training examples of objects in each class.

We further compare the scaling tendency of our approach with the one reported for a non-hierarchical representation by Opelt et al. [3]. The comparison is given in Fig. 12 (a) where the worst case is taken as in [3]. We compare the size of the class-specific vocabulary at layer 5, where the learned compositions are of approximately the same granularity as the features used in [3]. We additionally compare the overall size of the vocabulary (a sum of the sizes over all layers). Our approach achieves a substantially better scaling tendency, which is due to sharing at multiple layers of representation. This, on the one hand, compresses the overall representation, while it also attains a higher variability of the compositions in the higher layers and consequently, a lower number of them are needed to represent the classes.

Fig. 12 (d) shows the storage demands as a function of the number of learned classes. This is the actual size of the vocabulary stored on a hard disk. Notice that the 15-class hierarchy takes only 1.6Mb on disk.

*Inference time.* We further test how the complexity of inference increases with each additional class learned. We randomly sample ten images per class and report the detection times averaged over all selected images. The times are reported as a function of the number of learned classes. The results are plotted in Fig. 12 (c), showing that the running times are significantly faster than the “worst case” (the case of independent class representation, in which each separate class vocabulary is used to detect objects). It is worth noting, that it takes only 16 seconds per image to apply a vocabulary of all 15 classes.

*Detection performance.* We additionally test the multi-class detection performance. The results are presented in Table 4 and compared with the performance of the single class vocabularies. The evaluation was the following. For the single class case, a separate vocabulary was trained

on each class and evaluated for detection independently of other classes. For the multi-class case, a joint multi-class vocabulary was learned (as explained in Sec. 6.2.2) and detection was performed as proposed in Sec. 5.2, that is, we allowed for competition among hypotheses explaining partly the same regions in an image.

Overall, the detection rates are slightly worse in the multi-class case, although in some cases the multi-class case outperformed the independent case. The main reason for a slightly reduced performance is due to the fact that the representation is generative and is not trained to discriminate between the classes. Consequently, it does not separate similar classes sufficiently well and a wrong hypothesis may end up inhibiting the correct one. As part of the future work, we plan to also incorporate more discriminative information into the representation and increase the recognition accuracy in the multi-class case. On the other hand, the increased performance for the multi-class case for some objects is due to feature sharing among the classes, which results in better regularization and generalization of the learned representation.

## 7 SUMMARY AND CONCLUSIONS

We proposed a novel approach which learns a hierarchical compositional shape vocabulary to represent multiple object classes in an unsupervised manner. Learning is performed bottom-up, from small oriented contour fragments to whole-object class shapes. The vocabulary is learned recursively, where the compositions at each layer are combined via spatial relations to form larger and more complex shape compositions.

Experimental evaluation was two-fold: one that shows the capability of the method to learn generic shape structures from natural images and uses them for object classification, and another one that utilizes the approach in multi-class object detection. We have demonstrated a competitive classification and detection performance, fast inference even for a single class, and most importantly, a logarithmic growth in the size of the vocabulary (at least in the lower layers) and, consequently, scalability of inference complexity as the number of modeled classes grows. The observed scaling tendency of our hierarchical framework goes well beyond that of a flat approach [3]. This provides an important showcase that highlights learned hierarchical compositional vocabularies as a suitable form of representing a higher number of object classes.

## 8 FUTURE WORK

There are numerous directions for future work. One important aspect would be to include multiple modalities in the representation. Since many object classes have distinctive textures and color, adding this information to our model would increase the range of classes that the method could be applied to. Additionally, modeling texture could also boost the performance of our current model: since textured regions in an image usually have

a lot of noisy feature detections, they are currently more susceptible to false positive object detections. Having a model of texture could be used to remove such regions from the current inference algorithm. Another interesting possible way of dealing with this issue would be to use high quality bottom-up region proposals to either rescore our detections or be used in our inference. Using segmentation in detection has recently been shown as a very promising approach [72], [73], [48].

Part of our ongoing work is to make the approach scalable to a large number of object classes. To achieve this, several improvements and extensions are still needed. We will need to incorporate the discriminative information into the model (to distinguish better between similar classes), make use of contextual information to improve performance in the case of ambiguous information (small objects, large occlusion, etc) and use attention mechanisms to speed-up detection in large complex images. Furthermore, a taxonomic organization of object classes could further improve the speed of detection [46] and, possibly, also the recognition rates of the approach.

## ACKNOWLEDGMENTS

This research has been supported in part by the following funds: Research program Computer Vision P2-0214 (Slovenian Ministry of Higher Education, Science and Technology) and EU FP7-215843 project POETICON.

## REFERENCES

- [1] R. Fergus, P. Perona, and A. Zisserman, "Weakly supervised scale-invariant learning of models for visual recognition," *International J. of Computer Vision*, vol. 71, no. 3, pp. 273–303, March 2007.
- [2] A. Torralba, K. P. Murphy, and W. T. Freeman, "Sharing visual features for multiclass and multiview object detection," *IEEE Trans. Patt. Anal. and Mach. Intell.*, vol. 29, no. 5, pp. 854–869, 2007.
- [3] A. Opelt, A. Pinz, and A. Zisserman, "Learning an alphabet of shape and appearance for multi-class object detection," *International J. of Computer Vision*, vol. 80, no. 1, pp. 16–44, 2008.
- [4] J. Shotton, A. Blake, and R. Cipolla, "Multi-scale categorical object recognition using contour fragments," *IEEE Trans. Patt. Anal. and Mach. Intell.*, vol. 30, no. 7, pp. 1270–1281, 2008.
- [5] V. Ferrari, L. Fevrier, F. Jurie, and C. Schmid, "Groups of adjacent contour segments for object detection," *IEEE Trans. Patt. Anal. and Mach. Intell.*, vol. 30, no. 1, pp. 36–51, 2008.
- [6] B. Leibe, A. Leonardis, and B. Schiele, "Robust object detection with interleaved categorization and segmentation," *International J. of Computer Vision*, vol. 77, no. 1-3, pp. 259–289, 2008.
- [7] G. Bouchard and B. Triggs, "Hierarchical part-based visual object categorization," in *CVPR*, 2005, pp. 710–715.
- [8] S. Ullman and B. Epshtein, *Visual Classification by a Hierarchy of Extended Features*, ser. Towards Category-Level Object Recognition. Springer-Verlag, 2006.
- [9] S. Fidler, M. Boben, and A. Leonardis, "Learning hierarchical compositional representations of object structure," in *Object Categorization: Computer and Human Vision Perspectives*, S. Dickinson, A. Leonardis, B. Schiele, and M. J. Tarr, Eds. Cambridge University Press, 2009.
- [10] S. Zhu and D. Mumford, "A stochastic grammar of images," *Foundations and Trends in Computer Graphics and Vision*, vol. 2, no. 4, pp. 259–362, 2006.
- [11] S. Fidler and A. Leonardis, "Towards scalable representations of visual categories: Learning a hierarchy of parts," in *CVPR*, 2007.
- [12] B. Ommer and J. M. Buhmann, "Learning the compositional nature of visual objects," in *CVPR*, 2007.
- [13] R. Girshick, P. Felzenszwalb, and D. McAllester, "Object detection with grammar models," in *NIPS*, 2009.



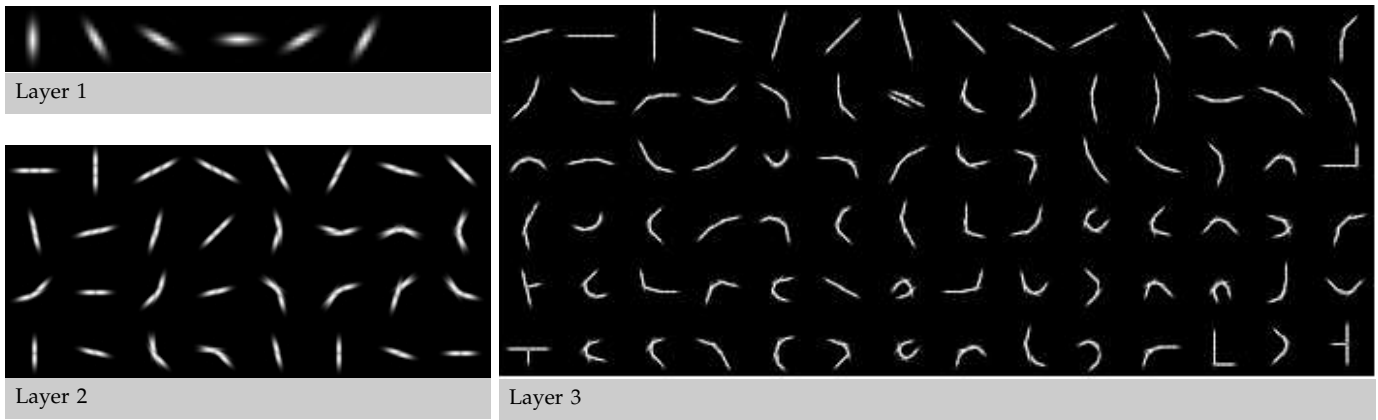


Fig. 8. Examples of learned vocabulary compositions (with the exception of a fixed Layer 1) learned on 1500 natural images. Only the mean of the compositions are depicted.



Fig. 9. Examples of samples from compositions at layers 4, 5, and top, object layer learned on 15 classes.

TABLE 2  
Information on the datasets used to evaluate the detection performance.

dataset	ETH shape					UIUC		Weizmann	INRIA	TUD	
class	Apple logo	bottle	giraffe	mug	swan	car_side (multiscale)		horse (multiscale)	horse	motorbike	
# train im.	19	21	30	24	15	40		20	50	50	
# test im.	21	27	57	24	17	108		228	290	115	

dataset	GRAZ										
class	bicycle_side	bottle	car_front	car_rear	cow	cup	face	horse_side	motorbike	mug	person
# train im.	45	/	20	50	20	16	50	30	50	/	19
# test im.	53	64	20	400	65	16	217	96	400	15	19

[14] J. K. Tsotsos, "Analyzing vision at the complexity level," *Behavioral and Brain Sciences*, vol. 13, no. 3, pp. 423–469, 1990.

[15] Y. Amit, *2d Object Detection and Recognition: Models, Algorithms and Networks*. MIT Press, Cambridge, 2002.

TABLE 3

Detection results. On the ETH shape and INRIA horses we report the detection-rate (in %) at 0.4 FPPI averaged over five random splits train/test data. For all the other datasets the results are reported as recall at equal-error-rate (EER).

	class	[50]	[68]	our approach
ETH shape	applelogo	83.2 (1.7)	89.9 (4.5)	87.3 (2.6)
	bottle	83.2 (7.5)	76.8 (6.1)	<b>86.2 (2.8)</b>
	giraffe	58.6 (14.6)	90.5 (5.4)	83.3 (4.3)
	mug	83.6 (8.6)	82.7 (5.1)	<b>84.6 (2.3)</b>
	swan	75.4 (13.4)	84.0 (8.4)	78.2 (5.4)
	<b>average</b>	76.8	84.8	83.7
INRIA	horse	84.8 (2.6)	/	<b>85.1 (2.2)</b>

	class	related work		our approach
UIUC	car_side, multiscale	90.6 [63]	93.5 [66]	<b>93.5</b>
Weizmann	horse_multiscale	89.0 [4]	93.0 [71]	<b>94.3</b>
TUD	motorbike	87 [6]	88 [37]	83.2

	class	[3]	[4]	our approach
GRAZ	face	96.4	97.2	94
	bicycle_side	72	67.9	68.5
	bottle	91	90.6	89.1
	cow	100	98.5	96.9
	cup	81.2	85	<b>85</b>
	car_front	90	70.6	76.5
	car_rear	97.7	98.2	97.5
	horse_side	91.8	93.7	<b>93.7</b>
	motorbike	95.6	99.7	93.0
	mug	93.3	90	90
	person	52.6	52.4	<b>60.4</b>

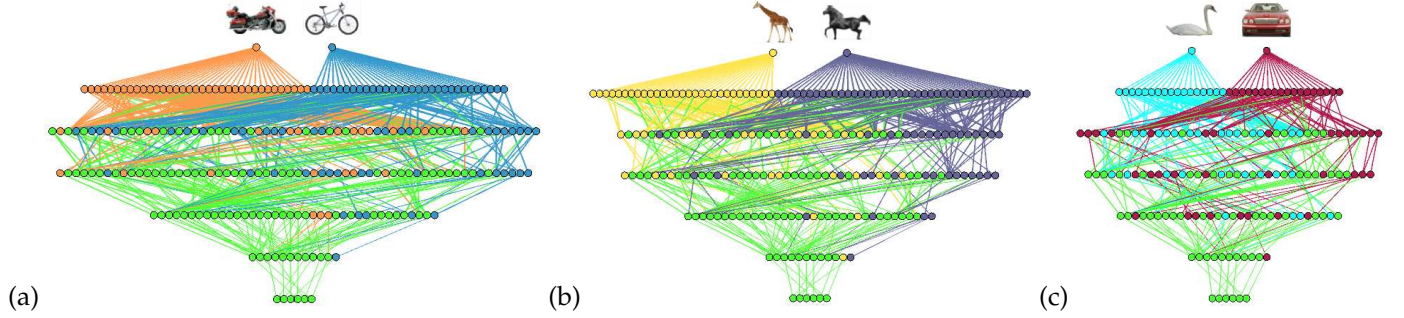


Fig. 10. Sharing of compositions between classes. Each plot shows a *vocabulary* learned for two object classes. The bottom nodes in each plot represent the 6 edge orientations, one row up denotes the learned second layer compositions, etc. The sixth row (from bottom to top) are the whole-shape, object-layer compositions (i.e., different aspects of objects in the classes), while the top layer is the class layer which pools the corresponding object compositions together. The green nodes denote the *shared* compositions, while specific colors show class-specific compositions. *From left to right*: Vocabularies for: (a) two visually similar classes (motorbike and bicycle), (b) two semi-similar object classes (giraffe and horse), (c) two visually dissimilar classes (swan and car\_front). Notice that even for dissimilar object classes, the compositions from the lower layers are shared between them.

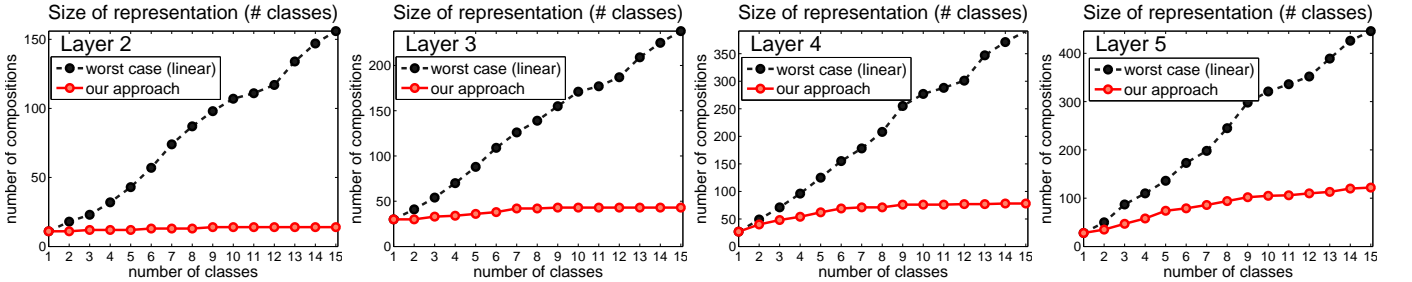


Fig. 11. Size of representation (the number of compositions per layer) as a function of the number of learned classes. “Worst case” denotes the sum over the sizes of single-class vocabularies.

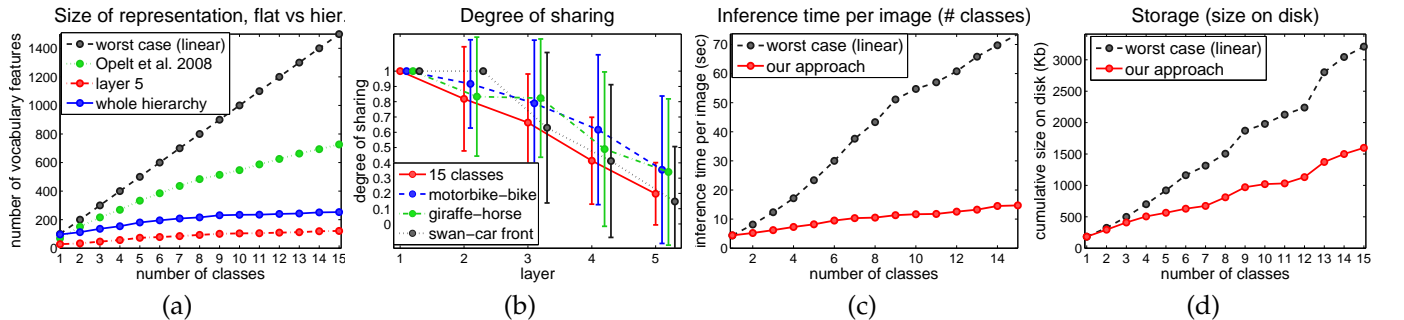


Fig. 12. From left to right: (a) A comparison in scaling to multiple classes of the approach by Opelt et al. [3] (flat) and our hierarchical approach; (b) Degree of sharing for the multi-class vocabulary; (c) Average inference time per image as a function of the number of learned classes; (d) Storage (size of the hierarchy stored on disk) as a function of the number of learned classes.

TABLE 4

Comparison in detection accuracy for single- and multi-class object representations and detection procedures.

class	Apple	bottle	giraffe	mug	swan	horse	cow	mbike	bicycle	car_front	car_side	car_rear	face	person	cup
measure	detection rate (in %) at 0.4 FPPI					recall (in %) at EER									
single	88.6	85.5	83.5	84.9	75.8	84.5	96.9	83.2	68.5	76.5	97.5	93.5	94.0	60.4	85.0
multi	84.1	80.0	80.2	80.3	72.7	82.3	95.4	83.2	64.8	82.4	93.8	92.0	93.0	62.5	85.0

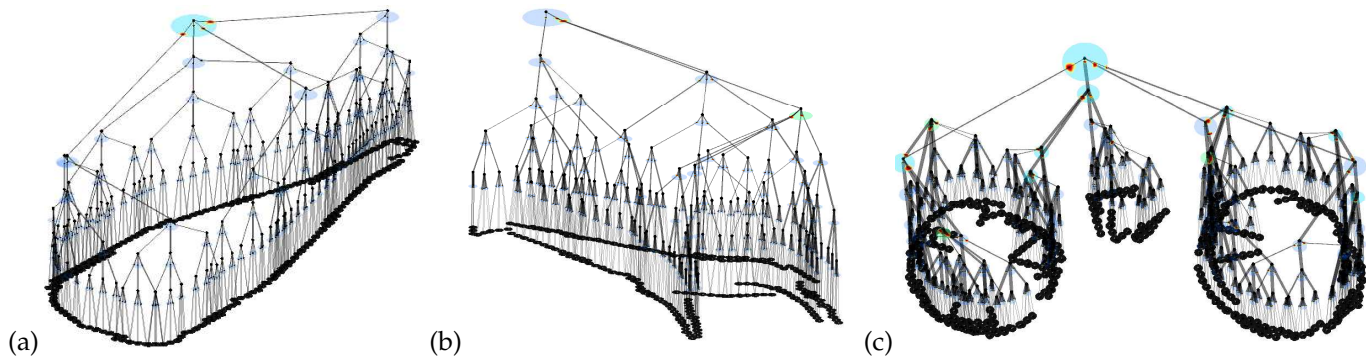


Fig. 13. One learned object-layer composition  $\omega^O$  for (a) *bottle*, (b) *giraffe*, and (c) *bicycle*, with the complete model structure shown. The blue patches denote the limiting circular regions, the color regions inside them depict the spatial relations (Gaussians). The nodes are the compositions in the vocabulary. Note that each composition models the distribution over the compositions from the previous layer for the appearance of its parts. For clarity, only the most likely composition for the part is decomposed further.

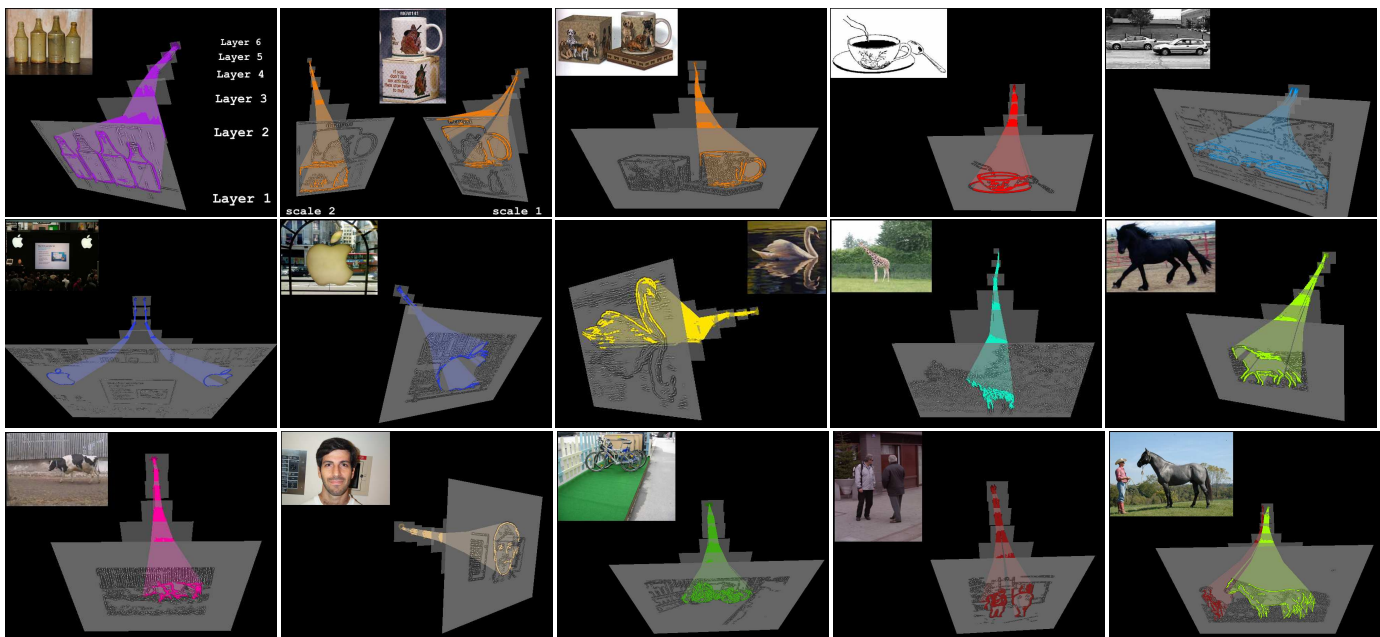


Fig. 14. Examples of detections. The links show the most probable hidden state activation for a particular (top-layer) class detection. The links are color-coded to denote different classes.

- [16] S. Fidler, M. Boben, and A. Leonardis, "Evaluating multi-class learning strategies in a generative hierarchical framework for object detection," in *NIPS*, 2009.
- [17] M. Leordeanu, R. Sukhtankar, and M. Hebert, "Object and category recognition from pairwise relations between features," in *CVPR*, 2007.
- [18] A. Shokoufandeh, L. Bretzner, D. Macrini, M. Demirci, C. Jonsson, and S. Dickinson, "The representation and matching of categorical shape," *Computer Vision and Image Understanding*, vol. 103, pp. 139–154, 2006.
- [19] S. Sarkar and K. Boyer, *Computing Perceptual Organization in Computer Vision*. Singapore: World Scientific, 1994.
- [20] S. Geman, D. Potter, and Z. Chi, "Composition systems," *Quarterly of Applied Mathematics*, vol. 60, no. 4, pp. 707–736, 2002.
- [21] J. Schwartz and P. Felzenszwalb, "Hierarchical matching of deformable shapes," in *CVPR*, 2007.
- [22] S. Edelman, N. Intrator, and J. S. Jacobson, "Unsupervised learning of visual structure," in *Biologically Motivated Computer Vision*, 2002, pp. 629–642.
- [23] M. Wertheimer, "Untersuchungen zur lehre von der gestalt." *Psychologische Forschung: Zeitschrift fuer Psychologie und ihre Grenzwissenschaften*, vol. 4, no. 1, pp. 301–350, 1923.
- [24] G. J. Ettinger, "Hierarchical object recognition using libraries of parameterized model sub-parts," MIT, Tech. Rep., 1987.
- [25] S. Dickinson, "The evolution of object categorization and the challenge of image abstraction," in *Object Categorization: Computer and Human Vision Perspectives*, S. Dickinson, A. Leonardis, B. Schiele, and M. J. Tarr, Eds. Cambridge University Press, 2009.
- [26] J. Utans, "Learning in compositional hierarchies: Inducing the structure of objects from data," in *NIPS*, 1994, pp. 285–292.

- [27] K. Fukushima, S. Miyake, and T. Ito, "Neocognitron: a neural network model for a mechanism of visual pattern recognition," *IEEE Systems, Man and Cyber.*, vol. 13, no. 3, pp. 826–834, 1983.
- [28] M. Riesenhuber and T. Poggio, "Hierarchical models of object recognition in cortex," *Nature Neuroscience*, vol. 2, no. 11, pp. 1019–1025, 1999.
- [29] T. Serre, L. Wolf, S. Bileschi, M. Riesenhuber, and T. Poggio, "Object recognition with cortex-like mechanisms," *IEEE Trans. Patt. Anal. and Mach. Intell.*, vol. 29, no. 3, pp. 411–426, 2007.
- [30] T. Masquelier and S. J. Thorpe, "Unsupervised learning of visual features through spike timing dependent plasticity," *PLoS Computational Biology*, vol. 3, no. 2, pp. 832–838, 2007.
- [31] M. A. Ranzato, F. J. Huang, Y. L. Boureau, and Y. LeCun, "Unsupervised learning of invariant feature hierarchies with applications to object recognition," in *CVPR*, 2007.
- [32] K. Jarrett, K. Kavukcuoglu, M. A. Ranzato, and Y. LeCun, "What is the best multi-stage architecture for object recognition?" in *ICCV*, 2009.
- [33] G. E. Hinton, "Learning multiple layers of representation," *Trends in Cognitive Sciences*, vol. 11, no. 10, pp. 428–434, 2007.
- [34] H. Lee, R. Grosse, R. Ranganath, and A. Y. Ng, "Convolutional deep belief networks for scalable unsupervised learning of hierarchical representations," in *ICML*, 2009, pp. 609–616.
- [35] E. Sudderth, A. Torralba, T. Freeman, and A. Willsky, "Describing visual scenes using transformed objects and parts," *International J. of Computer Vision*, vol. 77, no. 1-3, pp. 291–330, 2008.
- [36] B. Epshtein and S. Ullman, "Semantic hierarchies for recognizing objects and parts," in *CVPR*, 2007.
- [37] K. Mikolajczyk, B. Leibe, and B. Schiele, "Multiple object class detection with a generative model," in *CVPR*, 2006, pp. 26–36.
- [38] S. Todorovic and N. Ahuja, "Unsupervised category modeling, recognition, and segmentation in images," *IEEE Trans. Patt. Anal. and Mach. Intell.*, vol. 30, no. 12, 2008.
- [39] F. Scalzo and J. H. Piater, "Statistical learning of visual feature hierarchies," in *Workshop on Learning, CVPR*, 2005.
- [40] F. Fleuret and D. Geman, "Coarse-to-fine face detection," *International J. of Computer Vision*, vol. 41, no. 1/2, pp. 85–107, 2001.
- [41] L. Zhu, C. Lin, H. Huang, Y. Chen, and A. Yuille, "Unsupervised structure learning: Hierarchical recursive composition, suspicious coincidence and competitive exclusion," in *ECCV*, vol. 2, 2008, pp. 759–773.
- [42] Y. Amit, D. Geman, and X. Fan, "A coarse-to-fine strategy for multiclass shape detection," *IEEE Trans. Patt. Anal. and Mach. Intell.*, vol. 26, no. 12, pp. 1606–1621, 2004.
- [43] Y. Amit and D. Geman, "A computational model for visual selection," *Neural Computation*, vol. 11, no. 7, pp. 1691–1715, 1999.
- [44] M. Marszałek and C. Schmid, "Constructing category hierarchies for visual recognition," in *ECCV*, ser. LNCS, vol. IV. Springer, 2008, pp. 479–491.
- [45] P. Zehnder, E. K. Meier, and L. V. Gool, "An efficient shared multi-class detection cascade," in *BMVC*, 2008.
- [46] S. Fidler, M. Boben, and A. Leonardis, "A coarse-to-fine taxonomy of constellations for fast multi-class object detection," in *ECCV*, 2010, pp. 687–700.
- [47] A. Krizhevsky, I. Sutskever, and G. E. Hinton, "Imagenet classification with deep convolutional neural networks," in *NIPS*, 2012, pp. 1106–1114.
- [48] R. Girshick, J. Donahue, T. Darrell, and J. Malik, "Rich feature hierarchies for accurate object detection and semantic segmentation," in *CVPR*, 2014.
- [49] R. C. Nelson and A. Selinger, "Large-scale tests of a keyed, appearance-based 3-d object recognition system," *Vision Research*, vol. 38, no. 15-16, pp. 2469–2488, 1998.
- [50] V. Ferrari, L. Fevrier, F. Jurie, and C. Schmid, "Accurate object detection with deformable shape models learnt from images," in *CVPR*, 2007.
- [51] R. Fergus, P. Perona, and A. Zisserman, "A sparse object category model for efficient learning and exhaustive recognition," in *CVPR*, vol. 1, 2005, pp. 380–397.
- [52] S. Fidler, M. Boben, and A. Leonardis, "Optimization framework for learning a hierarchical shape vocabulary for object class detection," in *BMVC*, 2009.
- [53] S. Fidler, G. Berginc, and A. Leonardis, "Hierarchical statistical learning of generic parts of object structure," in *CVPR*, 2006, pp. 182–189.
- [54] S. Fidler, M. Boben, and A. Leonardis, "Similarity-based cross-layered hierarchical representation for object categorization," in *CVPR*, 2008.
- [55] P. Felzenszwalb, R. Girshick, D. McAllester, and D. Ramanan, "Object detection with discriminatively trained part based models," *IEEE Trans. Patt. Anal. and Mach. Intell.*, vol. 32, no. 9, 2010.
- [56] N. Petkov, "Biologically motivated computationally intensive approaches to image pattern recognition," *Future Generation Computer Systems*, vol. 11, no. 4-5, pp. 451–465, 1995.
- [57] M. Weber, M. Welling, and P. Perona, "Towards automatic discovery of object categories," in *CVPR*, 2000, pp. 2101–2108.
- [58] S. Belongie, J. Malik, and J. Puzicha, "Shape matching and object recognition using shape contexts," *IEEE Transactions on Pattern Analysis and Machine Intelligence*, vol. 24, pp. 509–522, 2001.
- [59] S. Fine, Y. Singer, and N. Tishby, "The hierarchical hidden markov model: Analysis and applications," *Machine Learning*, vol. 32, no. 1, pp. 41–62, 1998.
- [60] L. Fei-Fei, R. Fergus, and P. Perona, "Learning generative visual models from few training examples: an incremental bayesian approach tested on 101 object categories," in *IEEE CVPR, Workshop on Generative-Model Based Vision*, 2004.
- [61] T. Joachims, "Making large-scale support vector machine learning practical," pp. 169–184, 1999.
- [62] H. Zhang, A. C. Berg, M. Maire, and J. Malik, "Svm-knn: Discriminative nearest neighbor classification for visual category recognition," in *CVPR*, vol. 2, 2006, pp. 2126–2136.
- [63] J. Mutch and D. G. Lowe, "Multiclass object recognition with sparse, localized features," in *CVPR*, 2006, pp. 11–18.
- [64] K. Yu, W. Xu, and Y. Gong, "Deep learning with kernel regularization for visual recognition," in *NIPS*, 2008, pp. 1889–1896.
- [65] A. Ahmed, K. Yu, W. Xu, Y. Gong, and E. P. Xing, "Training hierarchical feed-forward visual recognition models using transfer learning from pseudo tasks," in *ECCV*, vol. III, 2009, pp. 69–82.
- [66] N. Ahuja and S. Todorovic, "Connected segmentation tree – a joint representation of region layout and hierarchy," *CVPR*, 2008.
- [67] M. Varma and D. Ray, "Learning the discriminative power-invariance trade-off," in *ICCV*, 2007.
- [68] M. Fritz and B. Schiele, "Decomposition, discovery and detection of visual categories using topic models," in *CVPR*, 2008.
- [69] S. Maji and J. Malik, "Object detection using a max-margin hough transform," in *CVPR*, 2009.
- [70] B. Ommer and J. Malik, "Multi-scale object detection by clustering lines," in *ICCV*, 2009.
- [71] J. Shotton, A. Blake, and R. Cipolla, "Efficiently combining contour and texture cues for object recognition," in *BMVC*, 2008.
- [72] J. R. R. Uijlings, K. E. A. van de Sande, T. Gevers, and A. W. M. Smeulders, "Selective search for object recognition," *International J. of Computer Vision*, vol. 104, no. 2, 2013.
- [73] S. Fidler, R. Mottaghi, A. Yuille, and R. Urtasun, "Bottom-up segmentation for top-down detection," in *CVPR*, 2013.